Macromolecular Research

Article

DOI 10.1007/s13233-022-0052-6

www.springer.com/13233 pISSN 1598-5032 eISSN 2092-7673

Crystalline Phases Thermal Behaviour, Optical Energy Band Gap, and Broadband Radio Wave Frequency Dielectric Properties of PEO/PVDF Blend Films

Priyanka Dhatarwal
R. J. Sengwa*

Dielectric Research Laboratory, Department of Physics, Jai Narain Vyas University, Jodhpur - 342 005, India

Received January 16, 2022 / Revised February 22, 2022 / Accepted March 8, 2022

Abstract: Different composition ratios poly(ethylene oxide) (PEO) and poly(vinylidene fluoride) (PVDF) blend films (PEO/PVDF) were investigated by employing a differential scanning calorimeter (DSC), ultraviolet-visible (UV-Vis) spectrophotometer, and radio frequency impedance analyzer (RF-IA). Crystalline phases of the PEO and PVDF in the blends, their melting temperatures and the degree of crystallinity were determined using the DSC thermograms. These structural parameters of the semicrystalline polymers explain a significant alteration in heterogeneous chains interaction with the composition variation of the constituents in the PEO/PVDF blends. The UV-Vis range absorbance spectra of these blend films were reported and analyzed for the determination of their optical energy band gap values. The decreased band gap values of the polymer blends as compared to that of the pristine polymers evidenced a considerable structural disordering of the polymers functional groups which cause the creation of the localized states that assisted the electronic transitions. The RF range dielectric permittivity of the PEO/PVDF blend films showed a gradual decrease with sweeping the frequencies from 1 MHz to 1 GHz, but it enhanced anomalously at the starting frequencies when the PVDF amount was relatively increased in the polymer blend. The alternating current (AC) electrical conductivity of these blends exhibited a linear variation with the change of frequency, and it notably altered at a fixed frequency when the polymer composition ratio in the blend films was varied. These experimental results of the PEO/PVDF blend films are highly creditable to emerging polymer-based flexible technologies of radio-electronic and optoelectronic devices.

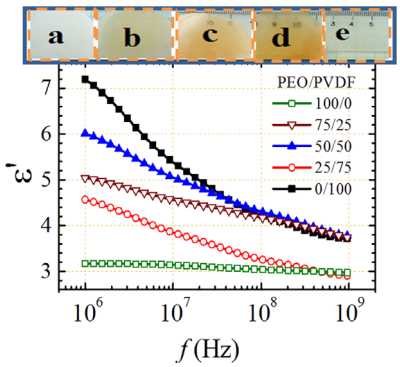

Keywords: PEO/PVDF blend, Crystalline phase, Thermal parameters, Energy band gap, RF dielectric properties.

1. Introduction

Polar polymer matrices of appreciable flexibility, affordable cost, lightweight, and good reproducible performance in the pristine form, blends, and their composites, all credited with the exponential growth of flexible-type electronic and electrical devices.[1-5] Among the synthetic polar polymers, the semicrystalline PEO material has hydrophilic and biodegradable character with excellent chain segmental dynamics, good solid solvent character for alkali metal salts, and outstanding film-formation ability by both the solution cast and melt-press methods.[6] All these valuable properties of the PEO matrix are ascribed to its low melting temperature and the presence of an ether oxygen functional group in the linear chain backbone. These promising properties of the PEO have established it as the most appropriate polymer matrix for the creation of a variety of ion-conducting solid polymer electrolyte (SPE) materials.[6-8] Such types of electrolytes have already been proven to be successful in the fabrication of all-solid-state ion-conducting devices, especially high-performance rechargeable batteries.[6] Additionally, the PEO matrix has been frequently considered in the progress of polymer nanocomposites (PNCs) for nanodielectric and optoelectronic applications.[9-13] Besides these useful properties of the PEO matrix, it has some drawbacks like poor thermal and mechanical stabilities, and also low optical transparency[12,13] which needs to be improved, by polymer blending and incorporation of additives, as briefly explained in the following part, to augment its massive technological uses.

In comparison to the important properties of the PEO matrix, the PVDF matrix also has several creditable properties like high environmental inertness, stronger hydrophobicity, polymorphic crystalline character, appreciable optical transparency, and relatively high dielectric constant with low losses.[5,14-17] These promising properties accredited the PVDF matrix as a superior thermophysical and polar electro-active material for making a wide range of multifunctional composites in regards to energy harvesting and storage devices,[5,14-17] memory devices,[18] and several next-generation innovative devices.[19-21]

For the extensive technological uses of the polymer matrices, the polymer blend matrices demonstrate a greater revolution in developing advanced materials. The useful properties of

Acknowledgment: The UGC, New Delhi, is gratefully acknowledged for the SAP DRS-II grant No. F.530/12/DRS-II/2016 (SAP-I). One of the authors (PD) thanks to the CSIR, New Delhi for an award of the research grant through a postdoctoral fellowship.

***Corresponding Author:** R. J. Sengwa (rjsengwa@rediffmail.com, rjs.ph@jnvu.edu.in)

a polymer blend matrix can be classically optimized by adjusting the blended polymers composition ratios during state-of-the-art blend preparation with the green chemistry process.[22,23] Earlier studies categorized that the polymers in their blend may have either good miscibility or partial, depending on the polymer hydrophobic/hydrophilic character, the strength of heterogeneous interactions of the functional groups, and the difference in glass transition temperatures.[23] Besides the confirmation of polymer blend miscibility and related valuable parameters, there is a prime need to examine and optimize the other useful properties, and also their dependency on the blend polymer composition ratio to realize the blend matrix for advanced technological uses.[22–24] Detailed study of structural, morphological, rheological, and thermal properties of the polymer blends is important from an academic and materials engineering point of view.[22,23] But the optical and dielectric characterization of individual polymers and the blend of polymers endorsed their numerous promising properties for industrial applications.[1-3] The dielectric and electrical properties of the polymeric materials are considered one of the key parameters to decide their usefulness as novel electrical insulators and dielectric substrates in the development of stretchable-type electronic devices that can suitably work under the influence of broadband frequency electric field.[1,5,9-12,18,20,24-27]

In regards to characterization and optimization of the functional properties of polymer blends, a blend of the PEO with PVDF outcomes was partially miscible, but the degree of miscibility varies reasonably when the polymers compositional ratio was changed.[28-30] Besides the partial miscibility of the PEO and PVDF in the PEO/PVDF blend, it is often used as a host matrix for the preparation of novel functional polymer nanocomposites with the inclusion of appropriate inorganic/organic nanomaterials,[31-34] and also in the development of a wide range promising SPEs for ion-conducting devices.[35-41]

Recently, we have characterized in detail the compositional ratios dependent morphological, elemental percentage, and structural properties of the PEO/PVDF blend films using SEM, EDX, XRD, and FTIR techniques whereas the low-frequency range dielectric and electrical properties were explored by employing the precision LCR meter.[30] With the usable structural characteristics and the dielectric properties, we have also prepared and investigated the PEO/PVDF blend matrices-based several important PNCs[32-34] and the SPEs.[39-41]

But a survey of the literature infers that the comprehensive thermal parameters of the PEO and PVDF crystalline phases and their degree of crystallinity, the ultraviolet-visible (UV-Vis) wavelength range absorbance and the optical energy band gap, and especially the broadband radio frequency range dielectric behaviour of the PEO/PVDF blend films with the composition variation have yet to be investigated. The characterization of these properties of the PEO/PVDF blends is important from the fundamental and academic points of view and also to explore more industrial applications of such polymer blends. The dielectric measurement techniques are limited under the influence of high to ultrahigh range radio frequencies harmonic electric field, highly expensive, and have several difficult measurement protocols, and hence, the work on dielectric properties of polymers and their composites at ultrahigh radio frequencies is less attempted.[11,24,27,42-46] Although there is an intense industrial necessity of precisely laboratory-measured dielectric and electrical parameters of the polymeric materials with start frequency of some megahertz and extends up to several gigahertz.[2,11,24,27,43-47] In this framework, the present manuscript deals with the broadband radio frequencies dielectric and electrical behaviour of the PEO/PVDF blend films along with their optical properties and the detailed thermal parameters of the polymer crystalline phases.

2. Experimental

2.1. Materials

The polymer samples used in this work are the PEO (M_v= 600,000 g mol^{-1}) and the PVDF (M_w≃534,000 g mol^{-1}) which were obtained from Sigma-Aldrich Co. The *N*,*N*-dimethylformamide (DMF), for HPLC and spectroscopic grade, was purchased from Loba Chemie, India, and used as a common solvent for the preparation of PEO/PVDF blend films by solution cast method.

2.2. Preparation of PEO/PVDF blend films

The PEO/PVDF blend films having PEO to PVDF amounts in the composition ratios 100/0, 75/25, 50/50, 25/75, and 0/100, by weight percentage, were prepared through casting their homogeneous solutions. The required amounts of PEO and PVDF for the different compositional ratio PEO/PVDF blends were dissolved in DMF solvent through heating with continuous magnetic bar stirring. These homogenized polymer blend solutions were cast onto glass Petri dishes. Then by heating on a thermostated hot plate at about 70 ℃, the solvent was evaporated, and finally, the materials were turned into the PEO/PVDF blend films. The detailed procedure of the PEO/PVDF blend films preparation was described in the previous publication.[30] The manual tests like bending and twisting realize that these blend films are flexible and non-sticky.

2.3. Measurements

The thermograms of these polymer blend films were recorded by employing the Netzsch Polyma 214 differential scanning calorimeter (DSC) instrument which was controlled with the Netzsch Proteus® software. For DSC measurements, the sample in small pieces weighing about 7.0 mg, was taken in an aluminium pan covered with a pierced lid, and then it was heated in an Arena® furnace with nitrogen (N_2) flow at a rate of 40 mL/min. Second heating run DSC thermograms of the samples were recorded at a heating rate of 10 ℃/min for their thermal analysis. The previous thermal history of the samples was removed by the first heating run performed at the rate of 20 ℃/min.

The spectrophotometer of double beam geometry (Cary 60, Agilent Technologies, Inc.) was employed and operated in the ultraviolet-visible (UV-Vis) wavelength λ range from 200 nm to 800 nm with a wavelength accuracy of 1 nm. The scan speed was set at 600 nm/min to firstly record the baseline correc-

tion, and then the absorbance spectra of the PEO/PVDF blend films were collected. All the measurements were performed at ambient temperature and controlled with the Agilent Cary WinUV® software.

The RF impedance analyzer of harmonic electric field frequencies covering the range from 1 MHz to 1 GHz (Keysight Technologies, Inc., Model: E4991B) along with its compatible solid-material dielectric test fixture (Product No.: 16453A) controlled by E4991B-002 material measurement firmware, was used for broadband radio frequency dielectric measurements. Before the sample dielectric measurements, the test fixture was calibrated by keeping the electrodes open, short, and then mounting the load (Teflon) between the electrodes to comply with the ASTM standards. The real part ε' of complex dielectric permittivity ($\varepsilon^* = \varepsilon' - j\varepsilon''$) and the dielectric loss tangent (tanδ, that is the ratio of imaginary part to the real part of the complex permittivity ($\varepsilon''/\varepsilon'$)) of the PEO/PVDF films, at a fixed temperature of 20 ℃, were recorded as a function of electric field frequency.

3. Results and discussion

3.1. Crystalline phases and their melting temperatures

The DSC thermograms of different composition ratios PEO/PVDF blend films, in the temperature range from 35 ℃ to 200 ℃, are provided in Figure 1(a). The PEO film, denoted by 100/0 in the figure, has an intense endothermic peak centered at about 70 ℃ (highlighted by a vertical dashed line) which is assigned to its crystalline phase melting process.[11] The pristine PVDF film, labelled by 0/100, also has an endothermic peak of relatively less intensity. But it is a superimposed doublet peak of 161.7 ℃ and 165.6 ℃ (see inset of Figure 1(a)) which can be allocated to the melting temperatures of the α-phase and the β-phase crystallites respectively, revealing the polymorphic character of the PVDF film.[48-50]

It is noted from Figure 1(a) that the endothermic peak related to the PEO crystallites in the PEO/PVDF blend films has appeared considerably at a lower temperature than that of the pristine PEO film, and its intensity is reduced remarkably when the PEO amount decreased in these blends. Firstly, the decrease in intensity of the PEO endothermic peak is expected because when there is a relative decrease of the PEO amount and simultaneous increase of the PVDF amount in the PEO/PVDF blends resulted in the lessen of PEO crystallites. Secondly, the appearance of the endothermic peak of PEO at a lower temperature in the blend, in comparison to that of the pristine PEO, evidences that the PEO crystallites turns thermally weaker and also have a large thermal diversity as revealed from the broadening of the peak. Thirdly, the anomalous shifts of the endothermic peak with the decrease of PEO concentration in the blends also infer that there is uneven miscibility variation with the change of constituent concentration in the PEO/PVDF blends.

Significant alterations in the peak position on the temperature scale, and also in the intensity and shape of the PVDF endothermic doublet in the PEO/PVDF blends with the variation in blend composition ratio can also be noted from the inset of Figure 1(a). These alterations in both the intensities and positions of the PEO and PVDF endothermic peaks confirm a large modulation in the crystallites of these semicrystalline polymers and the related thermal processes when the compositional ratio of the PEO/PVDF blends was varied from 25/75 to 75/25 wt%. We propose that all these modifications in the crystallites of these semicrystalline polymers are caused by heterogeneous interactions developed between the functional groups of the PEO and the PVDF chains. Furthermore, the endothermic peaks of the PEO and the PVDF materials in their blends also support the results on crystalline structures of these polymers which were characterized from the XRD and FTIR measurements by us previously.[30]

To examine the comprehensive thermal behaviour of the crystalline phases of PEO and PVDF amounts blended in these

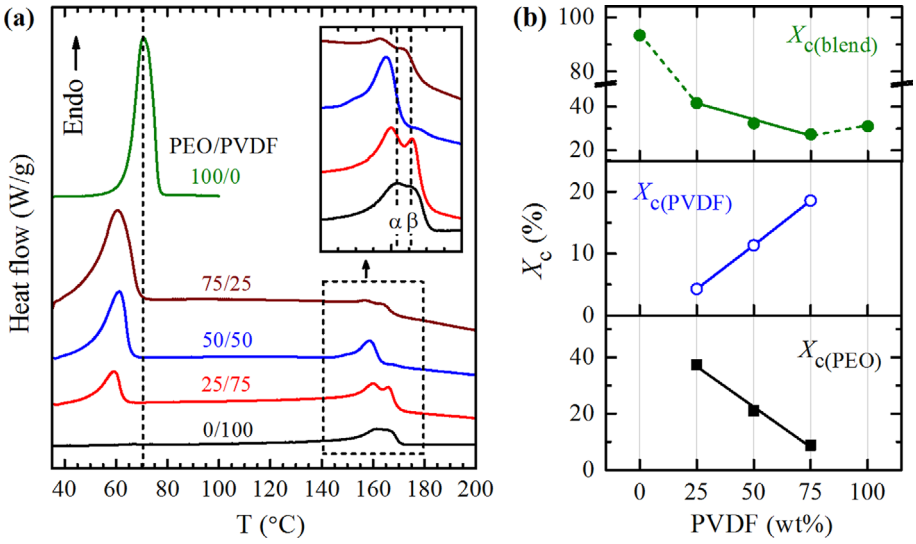

Figure 1. (a) DSC thermograms of the PEO/PVDF blend films with the PEO to PVDF composition ratios 100/0, 75/25, 50/50, 25/75, and 0/100 (wt/wt%), and (b) plots of the degree of crystallinity X_c of the PEO crystallites ($X_{c(PEO)}$), PVDF crystallites ($X_{c(PVDF)}$), and PEO/PVDF blend crystallites ($X_{c(blend)}$) versus PVDF (wt%) in the polymer blends. The inset of (a) shows the enlarged view of the endothermic peaks of the PVDF.

blend films, the values of various melting temperatures (T_m) related to the endothermic process were determined. These are the onset temperature $T_{m(O)}$, the peak temperature $T_{m(P)}$, and the end temperature $T_{m(E)}$, and also the temperature range for completion of the crystallites melting process $\Delta T_m = T_{m(E)} - T_{m(O)}$ and their values are listed in Table 1. The physical significance of these different temperature parameters related to the melting processes of crystalline phases in various semicrystalline polymers is explained in the previous literature.[11,51] In brief, the temperatures $T_{m(O)}$, $T_{m(P)}$, and $T_{m(E)}$ represents respectively, the start temperature of some crystallites melting process, the temperature of the maximum rate of crystallites melting, and the temperature at which the melting process of all the crystallites is fully completed.

The determination of ΔT_m values signify the temperature window over which the melting process of various thermal characteristic crystallites was completed. The higher ΔT_m means the polymer crystallites of a wider temperature range, and vice-versa. In other words, the ΔT_m values explain how the crystallites are thermally identical. If the ΔT_m is very narrow then it reflects that most of the crystallites are similar as far as their meting temperatures processes are considered. From Table 1, one can see that the ΔT_m value of the PEO crystallites is largely increased whereas that of the PVDF is significantly decreased for the 75/25 wt% of PEO/PVDF blend, which means the heterogeneous interactions influence the PEO and PVDF crystallites thermal diversely. This behaviour is further modified for the blend having of 50/50 wt% composition of the constituents. In this composition, the ΔT_m value of the PEO amount is yet higher than the pristine PEO but it is largely reduced for the PVDF amount as compared to the pristine PEO. When the blend is made of 25/75 wt%, the ΔT_m of PEO amount is found close to that of the pristine PEO and at the same time ΔT_m of the PVDF amount again increased. These temperature parameters of the PEO crystallites in the PEO/PVDF blends explain that there is some anomaly with changing the PEO concentration but relative lowering of $T_{m(P)}$ confirms a reduction in the thermal stability of the crystallites when the different amounts of PVDF were blended with varying the PEO amounts through the solution casting method. It has been noted from Table 1 that the values of melting temperatures for the α-phase and β-phase of the PVDF crystallites, respectively denoted by $T_{m(\alpha)}$ and $T_{m(\beta)}$, also reduced in the PEO/PVDF blends which illustrates a decrease in their thermal stabilities. These results on the melting temperatures of various crystalline phases confirm that the heterogeneous chain interaction weakens the thermal stability of PEO crystallites as well as that of the PVDF in the blends. Furthermore, the heterogeneous interactions strength are the blend composition concentration dependent, and effectively affected the melting nature of the PEO and that of the PVDF crystallites in the blends.

The values of crystalline melting enthalpy ΔH_m of the PEO and the PVDF in the PEO/PVDF blend samples were determined by taking the areas of corresponding endothermic peaks, and these are given in Table 1. Then from these ΔH_m values, the degree of crystallinity X_c(%) of the PEO and PVDF crystallites in the various composition ratio PEO/PVDF blends were determined from the enthalpy ratio relation $X_c(\%) = (\Delta H_m / \Delta H_{m0}) \times 100$. In this relation, ΔH_{m0} denotes the melting enthalpy values of the complete crystalline PEO material and that of the PVDF material, and these values are taken respectively 213.7 *J*/g and 104.7 *J*/g from the previous literature.[11,50,51] The obtained crystallinity values of the PEO and PVDF crystallites (which were denoted by $X_{c(PEO)}$ and $X_{c(PVDF)}$, respectively) in these blend samples along with the pristine polymers are recorded in Table 1 and also plotted against PVDF (wt%) in Figure 1(b). It can be noted from Table 1 that the pristine PEO film crystallinity (93.4 %) is three times high than that of the pristine PVDF film crystallinity (31.1%).

About the explanation of the crystallinity amount in the PEO/PVDF blend films with the change in blend composition ratio, firstly, it can be noted from the lower and middle layers of Figure 1(b) that there is a linear variation of the crystallinity of both the polymers with the change of PVDF amount in the blends. This finding suggests that the interactions between PEO and PVDF chains uniformly modulate the degree of crystallinity and it is ruled by the amounts of the polymers in the blends. Secondly, the values of the total degree of crystallinity of the PEO/PVDF blends, that is denoted by $X_{c(blend)}$ (%), are deduced by taking the arithmetic summation of $X_{c(PEO)}$ (%) and $X_{c(PVDF)}$ (%) values which are given in Table 1. The obtained $X_{c(blend)}$ (%) values of the PEO/PVDF blends are provided in Table 2. One can read from this table that the $X_{c(blend)}$ (%) values are 41.7, 32.4, and 27.3 respectively, for the 75/25, 50/50, and 25/75 (wt/wt%) com-

Table 1. Crystalline phase melting parameters (onset temperature $T_{m(O)}$, peak temperature $T_{m(P)}$, end temperature $T_{m(E)}$, and melting temperature range ΔT_m), enthalpy of melting ΔH_m, and percentage degree of crystallinity X_c of the PEO ($X_{c(PEO)}$) and PVDF ($X_{c(PVDF)}$) crystallites in the PEO/PVDF blend films of composition ratios 100/0, 75/25, 50/50, 25/75, and 0/100 (wt/wt%)

PEO/PVDF (wt/wt%)	$T_{m(O)}$ (°C)	$T_{m(P)}$ (°C)	$T_{m(E)}$ (°C)	ΔT_m (°C)	ΔH_m (J/g)	X_c (%)
PEO endothermic peak						
100/0	64.7	70.7	76.6	11.9	199.5	93.4
75/25	52.3	60.4	68.6	16.3	79.93	37.4
50/50	52.4	61.2	65.4	13.0	45.14	21.1
25/75	51.8	59.3	62.9	11.1	18.75	8.8
PVDF endothermic peaks						
75/25	153.1	156.9, 162.9	168.4	15.3	4.49	4.3
50/50	152.4	158.7	163.0	10.6	11.87	11.3
25/75	153.8	160.0, 165.9	169.5	15.7	19.42	18.5
0/100	154.0	161.7, 165.6	173.4	19.4	32.53	31.1

Table 2. The values of degree of crystallinity of the blend $X_{c(blend)}$, degree of crystallinity of the ideal blend $X_{c(blend)}^{(ideal)}$, and the deviation in crystallinity from ideal behaviour of the blend $\Delta X_{c(blend)}$ for the PEO/PVDF blend films of composition ratios 75/25, 50/50, and 25/75 (wt/wt%)

PEO/PVDF (wt/wt%)	$X_{c(blend)}$ (%)	$X_{c(blend)}^{(ideal)}$ (%)	$\Delta X_{c(blend)}$ (%)
75/25	41.7	77.8	−36.1
50/50	32.4	62.3	−29.9
25/75	27.3	46.6	−19.3

positions of the PEO to the PVDF in the blend films. Thirdly, the upper layer of Figure 1(b) explains that the $X_{c(blend)}$ values of the PEO/PVDF films also vary linearly with the change of blended polymer compositions, and it decreases when the PVDF amount increased in the blends. Fourthly, we noted from Tables 1 and 2 that the $X_{c(blend)}$ value (32.4%) of equal amounts polymers PEO/PVDF blend is close to that of the pristine PVDF film (31.1%), whereas the PVDF-rich amount PEO/PVDF film has it slightly lower. In contrast to this result, the PEO-rich amount PEO/PVDF blend film has $X_{c(blend)}$ value (41.7%) much lower than that of the pristine PEO film (93.4%). These outcomes evidenced that the crystallinity of the PEO is largely modified when initially a low amount of PVDF was blended with keeping a relatively high amount of the PEO. This finding also suggests that the thermally soft crystallites of the PEO (as recognized from the low melting temperature $T_{m(P)}$ = 70.7 ℃) are largely disturbed when blended with relatively hard crystallites of the PVDF (which are evidenced by their high melting temperature $T_{m(P)} \approx 165$ ℃). Lastly, it can be concluded that there is a dominant influence of PVDF interactions which largely modulate the PEO crystallites as compared to the PEO effect on the growth of PVDF crystallites through a solution cast preparation of the blend film.

To understand more about the crystallinity behaviour of these semicrystalline polymers blends, we propose that the blend crystallinity should obey the weight fraction-weighted additivity relation of the crystallinity of the pure polymer. According to the concept of an ideal blend, the total crystallinity of the ideal polymer blend $X_{c(blend)}^{(ideal)}$ can be computed by $X_{c(blend)}^{(ideal)} = X_{c(A)} W_A + X_{c(B)} W_B$, where $X_{c(A)}$ and $X_{c(B)}$ are the crystallinity of the pristine polymers *A* and *B* having the respective weight fractions W_A and W_B in the blend. Using this relation, the $X_{c(blend)}^{(ideal)}$ values were determined for the PEO/PVDF blends and reported in Table 2. These values are found respectively 77.8, 62.3, and 46.6 (%) for the 75/25, 50/50, and 25/75 (wt%) compositions of the PEO/PVDF blends. It is further noted that the $X_{c(blend)}^{(ideal)}$ values are significantly high than the $X_{c(blend)}$ values of the respective composition PEO/PVDF blends. Additionally, the deviation in crystallinity from the ideal behaviour of the blends $X_{c(blend)}$ (%) is computed from the relation $\Delta X_{c(blend)}$ (%) = $X_{c(blend)}$ (%) - $X_{c(blend)}^{(ideal)}$ (%). The obtained $\Delta X_{c(blend)}$ (%) values, reported in Table 2, are -36.1, -29.9, and -19.3 (%) respectively, for the 75/25, 50/50, and 25/75 (wt%) composition amounts in the PEO/PVDF blends. These negative $\Delta X_{c(blend)}$ (%) values of the blends evidence that the heterogeneous interaction between the functional groups of the polymers chains remarkably hinders the growth of PEO and PVDF crystallites during the preparation of the blends as compared to that grow in these pristine polymer films.

3.2. UV-Vis absorbance and energy band gap

The absorbance versus wavelength λ plots, in the UV-Vis wavelength range covering 200 nm to 800 nm, for the PEO/PVDF blend films are presented in Figure 2. This figure evidences that the PVDF film has comparatively low absorbance, over the entire experimental wavelength range, then that of the PEO film and also the PEO/PVDF blend films. This finding reveals better optical transparency of the PVDF film in comparison to the mild transparent character of the milky-type PEO film.[12,13] Further, the PEO/PVDF blend films also have poor transparency for visible range photons which is mainly due to the PEO amount in the blend films. The difference in the transparency of the PEO, PVDF, and PEO/PVDF blend films can also be seen with naked eyes from their digital pictures pasted in the upper layer of Figure 2. The milky PEO film (a) is opaque whereas the brownish to light brown PEO/PVDF blend films (b, c, d) are changed from opaque to a little transparent with an increase of PVDF amount in the blend composition. In comparison to these films, the pristine PVDF film (e) has relatively better transparency. The UV-Vis absorbance characteristics of the PEO/PVDF blend films seem consistent with the appearance of their digital pictures. Additionally, a steep rise in absorbance of the PEO film, and also that of the PVDF film, with the decrease in wavelength in the lower UV region attributes to the electronic transitions (*i.e.*, the jump of valence band electrons to the conduction band) which is the characteristic behaviour and well demonstrated for several types of polymeric materials.[12,13,25,52-55] The PEO/PVDF blend films also exhibited a relatively large rise in absorbance with the decrease in wavelength covering the entire experimental range

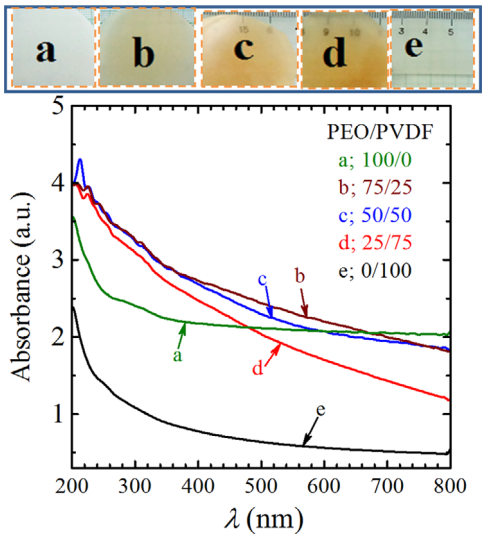

Figure 2. UV-Vis absorbance spectra of the PEO/PVDF blend films with PEO to PVDF compositional ratios 100/0, 75/25, 50/50, 25/75, and 0/100 (wt/wt%). The upper layer shows the digital picture of these films. The PEO film (a) is opaque, PEO/PVDF blend films (b, c, d) are changed from opaque to a little transparent with an increase of PVDF amount in the blend composition, and the PVDF film (e) has relatively better transparency with naked eyes.

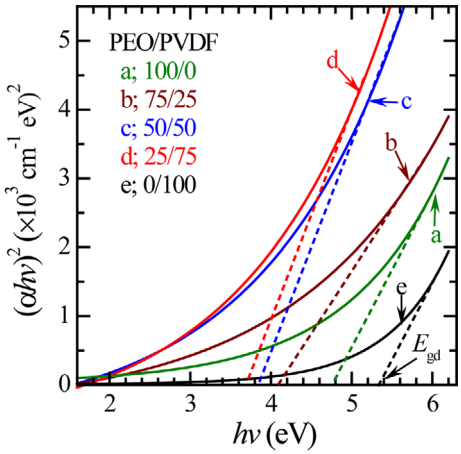

Figure 3. Tauc's plots of the PEO/PVDF blend films with PEO to PVDF compositional ratios 100/0, 75/25, 50/50, 25/75, and 0/100 (wt/wt%). Slanted dashed lines are the appropriate tangents drawn on the plots and extrapolated to the *x*-axis which give the band gap values corresponding to the zero value of the *y*-axis.

of the UV region.

The electronic transition behaviour with the variation in constituents composition of the PEO/PVDF blends can be explained better with the determination of their direct energy bandgap E_{gd} values using the Tauc's plots ($(\alpha h\nu)^2$ versus photons energy $h\nu$), depicted in Figure 3. The extrapolation of the tangents drawn on these plots was done (shown by slanted dashed lines) for estimation of E_{gd} values from the *x*-axis corresponding to the zero value of absorbance coefficient α on the *y*-axis *i.e.*, at $(\alpha h\nu)^2 = 0$, which is a common procedure used for the determination of energy band gap of the polymeric films.[12,13,25,26,55,56] The E_{gd} values of pristine PEO and PVDF films are found respectively 4.75 eV and 5.32 eV which are noted close to the earlier results on these polymers matrices-based different polymeric materials.[12,13,32,52] The PEO/PVDF blends have E_{gd} values 4.10 eV, 3.86 eV, and 3.65 eV corresponding to the constituent compositions 75/25, 50/50, and 25/75 (wt/wt%), which are significantly low in comparison to these pristine polymers. Further, it is noted that these E_{gd} values of the PEO/PVDF blends also decrease with the increase of the PVDF amount in the blends. The 25/75 wt% composition ratio PEO/PVDF blend has a band gap value close to that of several wide band gap metal oxides[25] which is highly interesting to this composition polymer blend for different semiconductor device applications.

The lowering in bandgap value of the polymer blends and the polymer composite materials is generally explained by the consideration of localized energy states in the forbidden energy bandgap. The structural disordering (some change in position of atoms and the associated arrangement of electric charges) occurs due to the constituents heterogeneous interactions mostly creating the localized energy states in the polymeric composites.[25,26,52-56] Relatively low bandgap values of these PEO/PVDF blend films explain that the heterogeneous interactions between the functional groups of the PEO and PVDF produced large defects in the electronic structures of these materials. As a result of this fact, there was a creation of some localized states in the forbidden energy bandgap of the blends which appreciably assisted the electronic transitions of the valence band electrons in the conduction band. Additionally, the variation in E_{gd} values with the change of polymer composition ratio in the PEO/PVDF blends infer that the width of localized states is also modulated with the blended amounts of these polymers.

3.3. Radio frequencies dielectric properties

Figure 4(a) demonstrates the dispersion of dielectric permittivity ε' and dielectric loss tangent tanδ values as a function of frequency *f* for the PEO/PVDF blend films covering the broad radio range electric field of 1 MHz to 1 GHz, and at a fixed temperature of 20 ℃. This figure showed that the pristine PEO film has low values of ε' and tanδ in comparison to that of the PVDF film, over the entire experimental radio frequency range. The ε' values of the PEO film displayed a little decrease, *i.e.*, from 3.18 to 2.97, when the frequency was increased in three orders of magnitude *i.e.*, from 1 MHz to 1 GHz. But at 1 MHz, the tanδ value of the PEO film is about 0.012, which exhibited a gradual increase when the frequency increased up to 100 MHz, and thereafter a noteworthy increase which reached the value up to 0.043 when the frequency of applied radio wave harmonic electric field was increased to 1 GHz. The critical range in which the ε' and tanδ values observed for the PEO film, recognizes this film as low permittivity and low loss dielectric material for the radio frequency electric field.[11,46]

In contrast to the low and stable dielectric permittivity of the PEO film in the wide radio frequency range, the PVDF film has a frequency-dependent and also relatively high ε' values (see Figure 4(a)). The ε' values of the PVDF film decreased from 7.18 to 3.79 with the increase of applied harmonic electric field frequency from 1 MHz to 1 GHz revealing a radio frequency tunable dielectric polarization behaviour of this electro-active polymeric material. The measured tanδ values of the PVDF film, depicted in the lower layer of Figure 4(a), changed from 0.107 to 0.067 corresponding to the start and end experimental frequencies and having a relaxation peak around 7 MHz with the tanδ value of 0.165, which can be assigned to the α-relaxation process of the chain motion.[17] In the polymers, the α-relaxation process represents the rotational and segmental motion of the C-C bonds in the polymer chain.[57] This α-relaxation process frequency shifts to about 20 MHz for the PVDF-rich amount PEO/PVDF blend film (25/75 wt%) but its peak intensity turned highly diffused suggesting that the interaction of PEO chains produce significant hindrance to the chain segmental motion of the PVDF chain. Furthermore, this chain segmental dynamical process is almost suppressed for the PEO/PVDF blend film having an equal composition ratio (50/50 wt%) of the blend polymers. Moreover, the increasing trend of tanδ values above 100 MHz for the PEO-rich amount PEO/PVDF blend film (75/25 wt%), and also that of the pristine PEO film (100/0 wt%) attributed to the existence of the dipolar relaxation process of the ether oxygen functional group which is consistent with the earlier reported around 1 GHz frequency span.[11]

Figure 4(a) also illustrates that the different compositional ratio PEO/PVDF blend films displayed the ε' and the tanδ val-

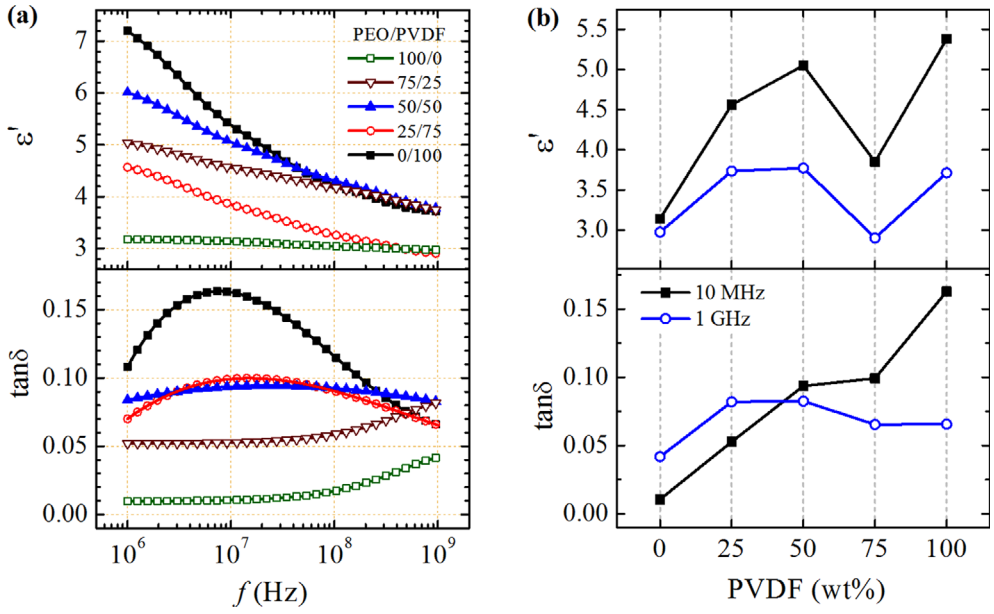

Figure 4. (a) The dielectric permittivity ε' and dielectric loss tangent tanδ spectra in the frequency range of 1 MHz to 1 GHz for the PEO/PVDF blends films with PEO to PVDF compositional ratios 100/0, 75/25, 50/50, 25/75, and 0/100 (wt/wt%), at 20 ℃, and (b) depicts variation of ε' and tanδ values of these blends against PVDF (wt%) at fixed frequencies of 10 MHz and 1 GHz.

ues in between that of the pristine PEO film and the PVDF film over the lower radio frequency region, covering the range from 1 MHz to 20 MHz. But in the high to ultrahigh radio frequency range, the ε' values for equal amounts constituents (50/50 wt%) blend and also that for the PVDF-rich blend (25/75 wt%) are observed nearly equal to that of the pristine PVDF film. In contrast to this result, the PEO-rich blend (75/25 wt%) exhibited the ε' values nearly equal to that of the pristine PEO film in the 200 MHz to 1 GHz ultra-high radio wave range. These results explain that the dipolar polarization depends on the type of polymers and also the compositional ratio of the polymers in the PEO/PVDF blends.

It is further noted that the tanδ values of PEO/PVDF blend films are appeared in between those of the pristine PEO film and the pristine PVDF film over a wider frequency range from 1 MHz to 300 MHz, and thereafter at higher frequencies (> 300 MHz) the blends tanδ values turned close to that of the PVDF film (see the lower layer of Figure 4(a)). The interesting feature noted from the tanδ values of the PVDF-rich and the PEO-rich these polymer blend films is that the variation in the dielectric loss function with the increase of frequency is insignificant covering the range from 1 MHz to about 100 MHz, whereas it remains almost steady over the entire frequency range for the PEO/PVDF blend film having an equal amount (50/50 wt%) of the PEO and PVDF polymers. These results explain that the dielectric loss part of the PEO/PVDF blends is almost independent of the harmonic electric field frequency, whereas their ε' values are found considerably tunable with the frequency. This finding confirms the suitability of these different compositions PEO/PVDF blend films as high-performance dielectric substrates for developing advanced flexible-type discrete or integrated electronic devices, and also as insulators for fabrication of energy storage capacitive devices workable over a broader range of radio frequencies. The significance of various types of polymeric materials, those were characterized in different frequency ranges, as dielectric and insulators in advances of flexible electronics is principally demonstrated in the previous literature.[1-5,11,17,45-47,58-66]

The PVDF concentration-dependent ε' and tan δ values of the PEO/PVDF blend films at fixed frequencies (*i.e.*, 10 MHz and 1 GHz) are shown in Figure 4(b). This figure illustrates a better understanding of the PEO/PVDF films dielectric behaviour with a varying composition ratio of the blended polymers. It can be noted from Figure 4(b) that the ε' values of PEO/PVDF blend films change monotonously, at both these fixed frequencies, with a variation of the concentration of the constituents in the blends. The tanδ values of these polymer blend films at 10 MHz showed an increase with the increase of PVDF amount, whereas at 1 GHz a minute anomalous variation is noted. These changes in the high-frequency dielectric parameters (ε' and tanδ) illustrate that there is a relative alteration in the strength of heterogeneous chains interaction as well as the dipolar ordering in the PEO/PVDF blends with the variation of blended polymers concentration.

3.4. AC electrical conductivity

The alternating current (AC) electrical conductivity (real part $\sigma' = \omega\varepsilon_0\varepsilon''$) versus frequency f plots of the PEO/PVDF blend films at a fixed temperature of 20 ℃ are depicted in Figure 5(a). All these plots showed an increase in σ' values with the increase of f confirming a strong dependency of conductivity on the frequency over a broad range of radio wave harmonic electric fields. Similar behaviour of the AC electrical conductivity as a function of wide range radio wave frequency was also reported previously for several other polymers and polymer-based nanocomposites.[11,43,46,66] Figure 5(a) further explains that the

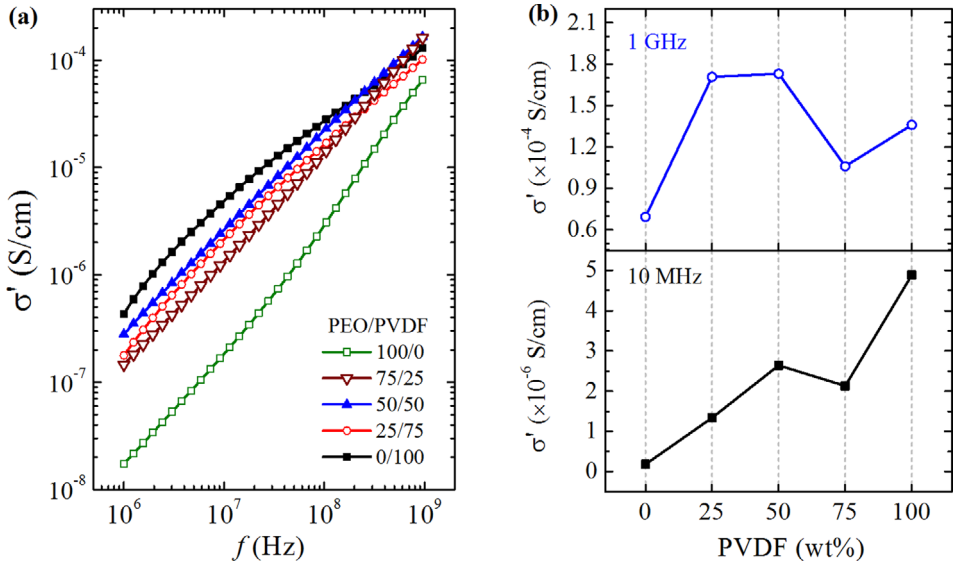

Figure 5. (a) The AC electrical conductivity σ' spectra in the frequency range of 1 MHz to 1 GHz for the PEO/PVDF blend films with PEO to PVDF compositional ratios 100/0, 75/25, 50/50, 25/75, and 0/100 (wt/wt%), at 20 ℃, and (b) depicts the variation of σ′ values of these blends against PVDF (wt%) at fixed frequencies of 10 MHz and 1 GHz.

PEO film has relatively low conductivity than the PVDF film over the entire experimental frequency range. Furthermore, at 1 MHz, the σ' is about one and a half order of magnitude high for the PVDF film than that of the PEO film which is due to relatively high dielectric losses in the PVDF material. This difference in σ' values of the PEO film and the PVDF film showing a gradual narrowing with an increase of frequency, and lastly reduced to about half an order of magnitude at 1 GHz. It is because there is a dominance effect of dipolar rotational losses in the PEO material whereas this effect suppresses in the PVDF material in the same frequency range as can be noted from the tanδ spectra of these materials (see Figure 4(a)). Additionally, it can also be seen that the σ' values of the PEO film and that of the PVDF film exhibited some non-linearity with an increase in frequency which is due to the occurrence of dielectric relaxation process in these polymers (chain segmental relaxation of PVDF in the experimental lower frequency range and the dipolar rotational relaxation of PEO in the higher frequency range). But the σ' values of the PEO/PVDF blend films increase almost linearly with an increase of frequency because they have either a weak relaxation process or it is completely suppressed. Additionally, the electrical conductivities of these PEO/PVDF blend films over the wider frequency range are found in between that of the PEO film and the PVDF film, but closer to that of the PVDF film, revealing the charge conduction mechanism is dominantly ruled by the PVDF structures in these blends.

Figure 5(b) illustrates the variation of σ' values of the PEO/PVDF blend films as a function of PVDF (wt%) in the blends, at selectively fixed frequencies of 10 MHz and 1 GHz. The σ' plot at 1 GHz reveals that the electrical conductivity has anomalous variation when the PVDF amount was increased in the PEO/PVDF blends which reflects some uneven changes in dipolar losses. But, at 10 MHz, the σ' values of the PEO/PVDF blends are less anomalous and they showed a linear rise with the increase of PVDF amount up to the 50 wt% in the blends.

To explore some correlation between the dielectric, electrical, optical, and thermal properties of the PEO/PVDF blends, herein firstly we compare the investigated these properties of the pristine PEO and PVDF materials. It is noted that the pristine PEO film has relatively low values of ε', σ', E_{gd}, and T_m whereas the high values of UV-Vis absorbance and X_c in comparison to that the pristine PVDF film. But the PEO/PVDF blend films have the ε' and σ' values in between the values of pristine polymers, absorbance close to the PEO film, X_c close to PVDF film, and E_{gd} relatively very low. Thus, it can be concluded that the dielectric and electrical properties of the PEO/PVDF blends are controlled by both the polymers, absorbance is predominantly ruled by the PEO whereas the X_c of the blend is mainly governed by the PVDF. In addition to these facts, the E_{gd} values of the blends significantly reduced which is effectively ruled by the heterogeneous interactions between the PEO and PVDF chains. Lastly, it can be reported that the prediction of a direct correlation between the dielectric, optical, and thermal properties of the PEO/PVDF blends is probable if these properties are compared with a series of various polymer blends having one of these polymers as a constituent of the blends.

4. Conclusions

This manuscript reports in detail, the PEO and the PVDF crystalline phases and their melting temperatures, and also the degree of crystallinity of these phases in the solution cast PEO/PVDF blend films covering the entire range of blend composition. Polymorphism of the PVDF (α-phase and β-phase) in the PEO/PVDF blend films largely alter with the change in blend composition whereas the degree of crystallinity of these polymer blend films decreased when the amount of PVDF was increased from 25 wt% to 75 wt%. The absorbance of UV-Vis electromagnetic radiations and the optical energy band gap studies on the PEO/PVDF blend films revealed that the heterogeneous chain

interaction produces effective localized states in the forbidden energy band gap, which promotes the electronic transition and thereby significantly reduces the band gap of these blend materials. The dispersion behaviour of the dielectric permittivity, dielectric loss tangent, and the AC electrical conductivity over the broadband radio frequency range (1 MHz to 1 GHz) for the PEO/PVDF blend films, at a fixed temperature of 20 ℃, is reported and thoroughly analyzed. The dielectric permittivity is found relatively high for the pristine PVDF film at the starting range frequencies and it largely decreased when the frequency of the applied radio wave harmonic electric field was increased. The PEO film has low permittivity and showed less alteration with sweeping the frequency of field from 1 MHz to 1 GHz range. The dielectric permittivity of the PEO/PVDF blend films is found effectively ruled by the PVDF amount in the blends. Furthermore, the AC electrical conductivity of these polymer blend films showed almost linear dependency with the variation of radio wave electric field frequencies. Appreciably the blend composition dependent thermal behaviour of the crystalline phases and also the optical, dielectric, and electrical properties of the PEO/PVDF blend films suggest that these blend materials could be potential candidates for various technological applications. Due to the flexible character of these polymer blends, they can serve as the stretchable and deformable-type dielectric substrate, electrical insulator, optical band gap controller, and UV-Vis shielding material in a wide range of emerging device technologies of the radio frequency electronics and also the optoelectronics.

Conflicts of interests: The authors declare that they have no known competing financial interests or personal relationships that could have appeared to influence the work reported in this paper.

Authorship contribution statement: Priyanka Dhatarwal: Conceptualization, Methodology, Data curation, Writing-original draft. **R. J. Sengwa:** Conceptualization, Supervision, Methodology, Data curation, Resources, Writing-original draft, Writing-review and editing.

References

(1) J. Wei and L. Zhu, *Prog. Polym. Sci.*, **106**, 101254 (2020).
(2) T. Tanaka and T. Imai, *Advanced Nanodielectrics: Fundamentals and Applications,* Pan Stanford Publishing Pte. Ltd., Singapore, 2017.
(3) G. D. Tabi, B. Nketia-Yawson, J. W. Jo, and Y. Y. Noh, *Macromol. Res.*, **28**, 1248 (2020).
(4) P. Sathiyanathan, D. M. Dhevi, A. A. Prabu, and K. J. Kim, *Macromol. Res.*, **27**, 743 (2019).
(5) D. Q. Tan, *J. Appl. Polym. Sci.*, **137**, e49379 (2020).
(6) Z. Xue, D. He, and X. Xie, *J. Mater. Chem. A*, **3**,19218 (2015).
(7) J. H. Yoon, W. J. Cho, T. H. Kang, M. Lee, and G.-R. Yi, *Macromol. Res.*, **29**, 509 (2021).
(8) R. Feng, B. Xu, N. S. Grundish, Y. Xia, Y. Li, C. Lu, Y. Liu, N. Wu, and J. B. Goodenough, *Angew. Chem.*, **60**, 17701 (2021).
(9) R. J. Sengwa and S. Choudhary, *J. Alloys Compd.*, **701**, 652 (2017).
(10) P. Dhatarwal, S. Choudhary, and R. J. Sengwa, *Polym. Bull.*, **78**, 2357 (2021).
(11) R. J. Sengwa and P. Dhatarwal, *J. Appl. Polym. Sci.*, **139**, 51599 (2021).
(12) M. A. Morsi, A. Rajeh, and A. A. Al-Muntaser, *Compos. Part B*, **173**, 106957 (2019).
(13) S. B. Aziz, R. B. Marif, M. A. Brza, A. N. Hassan, H. A. Ahmad, Y. A. Faidhalla, and M. F. Z. Kadir, *Results Phys.*, **13**, 102220 (2019).
(14) S. Nakazawa, Y. Matsuda, M. Ochiai, Y. Inafune, M. Yamato, M. Tanaka, and H. Kawakami, *Electrochim. Acta*, **394**, 139114 (2021).
(15) M. Wu, D. Liu, D. Qu, Z. Xie, J. Li, J. Lei, and H. Tang, *ACS Appl. Mater. Interfaces*, **12**, 52652 (2020).
(16) P. Sivaraj, K. P. Abhilash, B. Nalini, P. Perumal, K. Somasundaram, and P. C. Selvin, *Macromol. Res.*, **28**, 739 (2020).
(17) W. Zhou, T. Li, M. Yuan, B. Li, S. Zhong, Z. Li, X. Liu, J. Zhou, Y. Wang, H. Cai, and Z.-M. Dang, *Energy Stor. Mater.*, **42**, 1 (2021).
(18) H. Zhu, C. Fu, and M. Mitsuishi, *Polym. Int.*, **70**, 404 (2021).
(19) B. Jiang, J. Iocozzia, L. Zhao, H. Zhang, Y.-W. Harn, Y. Chen, and Z. Lin, *Chem. Soc. Rev.*, **48**, 1194 (2019).
(20) C. Tsonos, H. Zois, A. Kanapitsas, N. Soin, E. Siores, G. D. Peppas, E. C. Pyrgioti, A. Sanida, S. G. Stavropoulos, and G. C. Psarras, *J. Phys. Chem. Solids*, **129**, 378 (2019).
(21) B. S. Kim and J. Lee, *Chem. Eng. J.*, **301**, 158 (2016).
(22) L. A. Utracki and C. Wilkie, *Polymer Blend Handbook*, Springer Science+Business Media, Dordrecht, 2014.
(23) S. Thomas, Y. Grohens, and P. Jyotishkumar, *Characterization of Polymer Blends: Miscibility, Morphology and Interfaces*, Wiley-VCH Verlag GmbH & Co. KGaA, Weinheim, 2015.
(24) J. P. Runt and J. J. Fitzgerald, *Dielectric Spectroscopy of Polymeric Materials*, ACS, Washington, DC, 1997.
(25) R. J. Sengwa and P. Dhatarwal, *Opt. Mater.*, **113**, 110837 (2021).
(26) R. J. Sengwa and P. Dhatarwal, *J. Mater. Sci. Mater. Electron.*, **32**, 9661 (2021).
(27) F. Kremer and A. Schönhals, Eds., *Broadband Dielectric Spectroscopy*, Springer-Verlag, Berlin, 2003.
(28) M. N. Tamaňo-Machiavello, C. M. Costa, J. Molina-Mateo, C. Torregrosa-Cabanilles, J. M. M. Dueňas, S. N. Kalkura, S. Lanceros-Mendez, R. Sabater i Serra, and J. L. G. Ribelles, *Mater. Today Commun.*, **4**, 214 (2015).
(29) M. Mohamadi, M. Papila, H. Garmabi, and Z. G. Bajestani, *J. Appl. Polym. Sci.*, **136**, 48017 (2019).
(30) P. Dhatarwal and R. J. Sengwa, *Macromol. Res.*, **27**, 1009 (2019).
(31) R. S. Hafez, N. A. Hakeem, A. A. Ward, A. M. Ismail, and F. H. Abd El-kader, *J. Inorg. Organomet. Polym. Mater.*, **30**, 4468 (2020).
(32) R. J. Sengwa, P. Dhatarwal, and S. Choudhary, *Mater. Today Commun.*, **25**, 101380 (2020).
(33) P. Dhatarwal and R. J. Sengwa, *Mater. Res. Bull.*, **129**, 110901 (2020).
(34) P. Dhatarwal and R. J. Sengwa, *J. Polym. Res.*, **26**, 196 (2019).
(35) H. Wang, C. Lin, X. Yan, A. Wu, S. Shen, G. Wei, and J. Zhang, *J. Electroanal. Chem.*, **869**, 114156 (2020).
(36) Y. Mallaiah, V. R. Jeedi, R. Swarnalatha, A. Raju, S. N. Reddy, and A. S. Chary, *J. Phys. Chem. Solids*, **155**, 110096 (2021).
(37) E. E. Ushakova, A. V. Sergeev, A. Morzhukhin, F. S. Napolskiy, O. Kristavchuk, A. V. Chertovich, L. V. Yashina, and D. M. Itkis, *RSC Adv.*, **10**, 16118 (2020).
(38) K. K. Ganta, V. R. Jeedi, K. V. Kumar, and E. Laxmi Narsaiah, *Int. J. Polym. Anal. Char.*, **26**, 130 (2021).
(39) P. Dhatarwal and R. J. Sengwa, *Compos. Commun.*, **17**, 182 (2020).
(40) R. J. Sengwa and P. Dhatarwal, *Electrochim. Acta* **338**, 135890 (2020).
(41) P. Dhatarwal and R. J. Sengwa, *SN Appl. Sci.*, **2**, 833 (2020).
(42) S. Singha and M. J. Thomas, *IEEE Tran. Dielectr. Electric. Insul.*, **15**, 2 (2008).
(43) M. A. Olariu, C. Hamciuc, O.M. Neacsu, E. Hamciuc and L. Dimitrov, *Dig. J. Nanomater. Biostruct.*, **14**, 37 (2019).
(44) R. Moučka, M. Mravčáková, J. Vilčáková, M. Omastová, and P. Sáha, *Mater. Des.*, **32**, 2006 (2011).
(45) R. J. Sengwa and P. Dhatarwal, *Mater. Lett.*, **299**, 130081 (2021).
(46) P. Dhatarwal, R. J. Sengwa, and S. Choudhary, *J. Macromol. Sci. Part B:*

Phys., **61**, 111 (2022).
(47) W. Wei, X. Ren, S. Du, and F. Zhou, *IOP Conf. Ser.: Earth Environ. Sci.*, **714**, 032045 (2021).
(48) R. Gregorio Jr., *J. Appl. Polym. Sci.*, **100**, 3272 (2006).
(49) E. Brunengo, G. Luciano, G. Canu, M. Canetti, L. Conzatti, M. Castellano, and P. Stagnaro, *Polymer*, **193**, 122345 (2020).
(50) J. Sun, L. Yao, Q.-L. Zhao, J. Huang, R. Song, Z. Ma, L.-H. He, W. Huang, and Y.-M. Hao, *Front. Mater. Sci.*, **5**, 388 (2011).
(51) X. Zhao, S. Chen, J. Zhang, W. Zhang, and X. Wang, *J. Cryst. Growth*, **328**, 74 (2011).
(52) S. El-Sayed, Z. R. Farag, and S. Saber, *AIP Adv.*, **10**, 095127 (2020).
(53) F. M. Ali and F. Maiz, *Macromol. Res.*, **28**, 805 (2020).
(54) P. Dhatarwal and R. J. Sengwa, *Optik*, **233**, 166594 (2021).
(55) P. Dhatarwal, S. Choudhary, and R. J. Sengwa, *Indian J. Chem. Technol.*, **28**, 693 (2021).
(56) T. S. Soliman, M. M. Hessien, and Sh. I. Elkalashy, and J. Non-Cryst. Solids, **580**, 121405 (2020).
(57) J. K. Jung, Y. I. Moon, K. S. Chung, and K. T. Kim, *Macromol. Res.*, **28**, 596 (2020).
(58) Y. Liu, J. Gao, R. Yao, Y. Zhang, T. Zhao, C. Tang, and L. Zhong, *Mater. Chem. Phys.*, **250**, 123155 (2020).
(59) G. Zhang, Q. Li, E. Allahyarov, Y. Li, and L. Zhu, *ACS Appl. Mater. Interface*, **13**, 37939 (2021).
(60) S. C. Ryu, J. Y. Kim, C. Cho, and W. N. Kim, *Macromol. Res.*, **28**, 118 (2020).
(61) P. Chen, B. Chen, B. Qin, J. Wang, Q. Deng, and Y. Feng, *Macromol. Res.*, **29**, 589 (2021).
(62) A. Sanida, S. G. Stavropoulos, Th Speliotis, and G. C. Psarras, *Polymer*, **236**, 124311 (2021).
(63) Q. Li, J. Zhou, Y. Chen, X. Xia, M. Bo, Q. Deng, and Y. Feng, *Macromol. Res.*, **28**, 1261 (2020).
(64) L. S. Schadler and J. K. Nelson, *J. Appl. Phys.*, **128**, 120902 (2020).
(65) E. R. Radu, D. M. Panaitescu, L. Andrei, F. Ciuprina, C. A. Nicolae, A. R. Gabor, and R. Trusca, *Nanomaterials*, **12**, 95 (2022).
(66) R. J. Sengwa and P. Dhatarwal, *J. Phys. Chem. Solids*, **166**, 110708 (2022).

